James A. McNeil

MAKING LEMONADE: USING GRAFFITI TO DATE PETROGLYPHS

Petroglyphs, a form of rock art consisting of images pecked on rock surfaces, comprise one of the most important archaeological features of the Colorado Plateau region (Cole 2009). They provide glimpses into the life, behaviors, and customs of the prehistoric peoples who created them. Petroglyphs are widely distributed geographically and are composed of a broad sweep of themes relating to essentially everything of social significance to the people who created them. An important step in relating these images to other artifacts would be a reliable and non-destructive way of dating them.

For a review of rock art dating methods see Chapter 5 in Francis and Loendorf (2002). Relative dates can be discerned through superimposition and through relative levels of repatination although Dorn (2007) warns against this practice due to micro-environmental and other effects. Themes and styles can also provide approximate dates principally through associa-tion with dateable artifacts of similar theme located nearby. Direct physical dating of rock art has been attempted using a variety of methods including accelerator mass spectroscopy (AMS) measurements of ^{14}C, Particle-induced X-ray Excitation (PIXE), analysis of (K+Ca)/Ti cation ratios, and studies of micro-laminations in the desert varnish (Dorn 1989, 1994, 1998a, 1998b, 2007; Dorn and Oberlander 1981). There are some clear successes with these approaches, but some controversy as well (Beck et al. 1998). One major drawback to these methods is their cost and the requirement of a physical sample which damages the artifact.

Another approach makes use of the desert varnish, the dark pigment that accumulates on rock surfaces throughout the desert southwest. Desert varnish is unusually rich in manganese while the underlying base rock generally contains very little of it. Dorn and Oberlander (1981) found that the manganese accumulates through a metallogenic microbial process. Since the underlying rock is generally poor in manganese, the manganese in the desert varnish must arrive on the rock surface as dust from elsewhere which is then fixed by the metallogenic microbes. However, this process is poorly understood and other processes that transport Mn may be involved. Lytle et al. (2008) has developed a direct dating method based on portable X-ray fluorescence (XRF) measurements of manganese accumulation in petroglyphs. The hope is that if the manganese level can be correlated to known dates, one can estimate the age of the rock. The operating assumption of Lytle et al. is that when a glyph is pecked onto a rock surface, the patina is completely removed and the manganese accumulation process begins anew *at a constant rate*. However, as it is a biological process, growth rates are highly variable, depending on micro environmental conditions, moisture, dust, surface orientation and texture, over/underhang, etc. In addition, the pecked surfaces of petroglyphs are more susceptible to erosion and spalling—further complicating the picture.

Lytle et al. (2009) calibrated their XRF manganese measurements to dates determined though other methods including cosmogenic ^{10}Be and ^{26}Al levels as well as geologically significant events such as the Bonneville Flood (14,300 B.P.). They reported an approximately linear correlation between age and Mn accumulation. Their calibration curve extends to 35,000 B.P. with the youngest cosmogenic standards dating over 10,000 B.P. while their youngest geological standards are around 1500–2500 B.P. (much of these are systematically below their calibration line, however). They further claim that their

calibration line, corrected for surface slope effects, is universal, independent of location or base rock—a claim which seems problematic given the existence of rock faces that display high levels of local variability.

The purpose of this work is to determine the feasibility of using X-ray fluorescence (XRF) measurements of manganese in petroglyphs in the manner of Lytle et al., but using dated graffiti located on or adjacent to the petroglyph as a *local* calibration standard to estimate the age of the rock art. Unlike Lytle et al. we do not assume that the manganese accumulation rates are universal. The major limitation of this approach is that it can only be used under the special circumstances where the graffiti and target petroglyphs are superimposed or adjacent. Fortunately, the Colorado Plateau has several sites where these conditions are met. In this talk I present results for graffiti and petroglyphs found in the vicinities of Bluff and Moab, Utah.

The descriptions of the XRF device, the experimental procedures, data analysis methods, and the Sand Island petroglyph measurements were previously reported to the Comb Ridge Heritage Initiative Project, University of Colorado under contract to the BLM, Catherine M. Cameron, Principal Investigator. The "Dancing Bear" site results are new.

DESCRIPTION OF THE XRF DEVICE

X-ray fluorescence[1] (XRF) is widely used as an important tool in analytic materials research. XRF is the re-radiation (fluorescence) by atoms in the x-ray part of the spectrum following excitation. Atoms that are bombarded with primary x-rays or charged particles of sufficient energy can have inner shell electrons knocked out. When one of the atom's other electrons drops into the shell vacancy, it emits a (secondary) x-ray photon with an energy characteristic of the element. In this way the spectrum (number of photons as a function of energy) of the emitting atom can be used to identify it. In the case of manganese there are primarily two x-ray energies that can be used for identification, the so-called K_α and K_β x-rays at 5.90 keV and 6.49 keV, respectively. The red sandstone in the Colorado Plateau is rich in iron as well which has characteristic XRF photons at energies of 6.40 keV and 7.06 keV. As there is an experimental width of approximately 0.2 keV, the Mn K_β and Fe K_α spectra will overlap requiring that in the analysis both are taken into account simultaneously.

In order to detect very low levels of manganese in narrowly-pecked graffiti it was necessary to construct an XRF device, capable of being deployed in the field, with millimeter spatial resolution, and mounted on a stable platform that allows long collection times (~5-60 minutes). We assembled such a device from the following components:

1. AmpTek Mini-X, x-ray tube (Comet EDiX-40-4-Ag) with power supply and USB controller and software.
2. Ortec EASY-MCA-2K Multichannel Analyzer (MCA) with USB interface and MAESTRO-32 (TM) software.
3. AmpTek XR-100T x-ray detector and power supply with pulse shaping amplifier.
4. 12-V automobile battery with sine-wave inverter.
5. Tripod with boom and counterweight, mounting plate, +/- 20mm XY-translation stage.
6. Laptop PC, monitoring meters, and cables.

Figure 1 shows a schematic of the XRF device. The Mini-X and XR-100T were attached to an aluminum plate with their principal axes separated by 40 degrees. The XR-100T consists of a temperature-controlled 7 mm^2 Si-PIN detector with a thin Beryllium window. The detector produces Mn K_α peak widths of about 0.15 keV (full width at half maximum). In the field we found that the detector amplifier would drift slightly as the ambient temperature of the electronics bin changed. The high voltage and current of the

[1] For an introduction to XRF visit http://en.wikipedia.org/wiki/X-ray_fluorescence.

Mini-X can be adjusted from 10–40 kV and 5–200 μA, respectively (although the current at the higher voltages is limited to 100 μA). A custom collimator for the Mini-X was machined from brass to provide a narrow beam diameter of 1.58 mm. The Mini-X and XR-100T units were then mounted on an optical XY-translation stage which permitted sub-millimeter positioning of the x-ray beam on the target. Soft rubber tubing was fitted to the collimator tip to avoid any potential damage should it inadvertently come in contact with the petroglyph. Figure 2 shows the XRF head unit mounted on the tripod boom (without cables). To provide 120 VAC the battery was connected to a 150 W pure sine-wave inverter. The automobile battery capacity was about 50 A-hrs which was sufficient for about 6 hours of operation in the field. The tripod has a 1 m (~3') equilateral triangle base modified with one adjustable leg and a vertical extent of 3.5 m (~12'). The battery, inverter, power supplies, amplifiers, MCA, and USB hub were housed in a plastic crate with a lid to keep out dust and moisture. A 4.5 m (~15') custom cable bundle was constructed to connect the XRF unit to the electronic crate. The power supply and USB cable from the computer were then connected to the USB port and 120 VAC power in the electronic crate. In steady state the system (including the computer) drew about 4.5 A (54 W) from the battery.

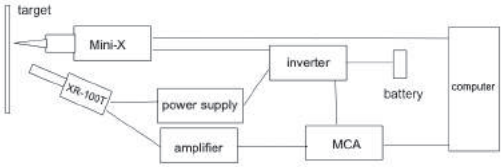

Figure 1. *Schematic of the XRF device.*

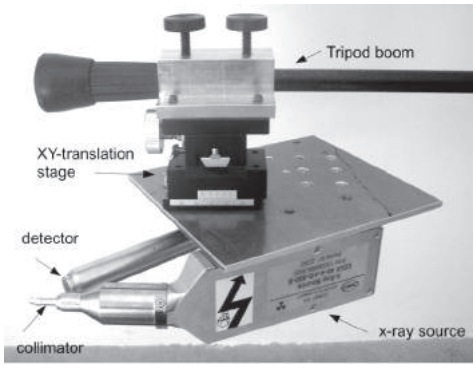

Figure 2. *Photograph of the XRF head unit showing the x-ray source and detector mounted on an XY-translation stage and boom.*

EXPERIMENTAL PROCEDURE

Before deploying the XRF device in the field, it was tested in the laboratory. Since we were focussed on the Mn–Fe energy region (5–7 keV), we set the high voltage on the Mini-X between 10–15 kV. To avoid data "pile up" (false double counts) while keeping the run times as low as possible, the current was adjusted between 15–100 μA such that the dead-time (signal processing "overhead") was about 1–3 percent. As a safety precaution, the CSM radiation safety officer inspected the device and surveyed the radiation in the vicinity of the device with a geiger area monitor to estimate the radiation exposures that could be expected and found very slight exposures could be expected. Nevertheless, standard precautions of shielding, distance, and time were adopted to minimize exposures, and radiation badges were used to monitor exposure levels.

For testing and calibration purposes a standard Mn target was fabricated by Dr. Joseph Beach of the CSM condensed matter group by depositing 158 nm of Mn on a glass slide. Using the sharp edge of this target, we determined the spatial resolution of the device to be less than 2.0 mm when fitted with the 1.58 mm-diameter collimator.

We adopted the following procedure in deploying the device in the field. Upon arrival at the site of the target glyph (graffiti/petroglyph), the tripod was set about 1 m from the rock face and one leg adjusted to have the tripod shaft be approximately vertical. The electronic crate was set near the base of the tripod and the computer set on a field table about 2 m away. The XRF head was then mounted on the tripod boom and vertically adjusted to be at the same level as the glyph and horizontally adjusted to be within about 2 cm of the glyph.

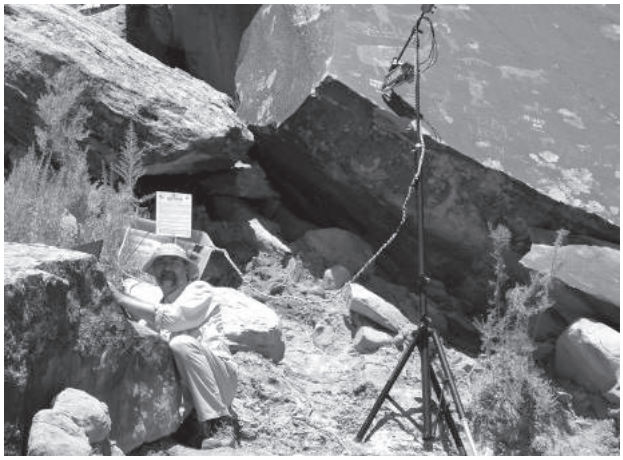

Figure 3. *XRF device deployed at the "Dancing Bear" panel near Moab, Utah.*

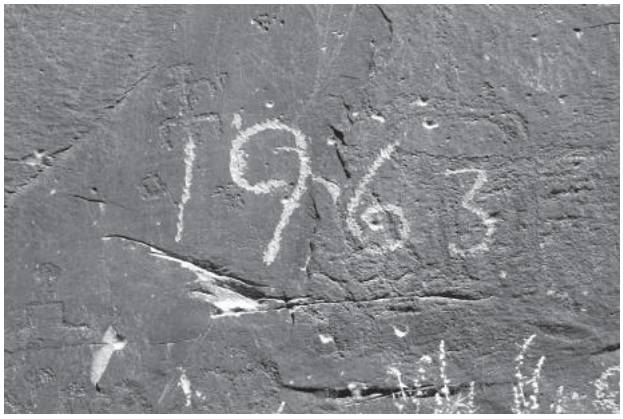

Figure 4. *Photograph of sample SI-1963a, Sand Island, Utah.*

The Mini-X interrupt jumper was installed, all cables connected, and the system powered up. Finally, the computer was booted up and the Mini-X controller and Maestro-32 (MCA) software launched. From the computer we set the Mini-X high voltage and current as well as the MCA live-time preset. The system was then tested for about 3–5 minutes using the standard thin-film Mn slide as the target. Each data run was recorded in Maestro's SPE-format which is ASCII readable. We made use of the live-time preset feature in the Maestro software to have runs of uniform duration, typically of 5–15 minutes. Figure 3 shows the device deployed at the "Dancing Bear" panel near Dewey Bridge north of Moab, Utah.

DESCRIPTION OF DATA COLLECTION

Graffiti/petroglyphs of Sand Island

The Sand Island petroglyph site is located on BLM land near Bluff, Utah. We received permission to conduct our experiments from the BLM Field Office, Monticello, Utah, and our work was supervised and monitored by archaeologist, Winston Hurst. (This portion of the work was supported in part by the Comb Ridge Initiative Heritage Project [Catherine Cameron, CU Boulder, Principal Investigator] and the description below is extracted from the resulting report.)

Sample SI-1963a–b. Prior to traveling to the region, we had identified several candidate panels at Sand Island that consisted of modern graffiti superimposed on or immediately adjacent to older petroglyphs. The first set of glyphs we measured, identified here as SI-1963a (the "3" of the "1963" graffito) and SI-1963b ("quadruped" petroglyph), is shown in Figure 4. It consists of a modern graffito "1963" superimposed on a big-horn sheep petroglyph of perhaps an archaic style.

We set up our apparatus following the procedure described in the previous section. We took seven 900-second measurements along a 2 cm section of the horizontal line in the "3" and along a parallel line directly above it within the petroglyph. In addition we took three 900-second measurements of the background patina directly above the petroglyph. We also took 300-second measurements of the Mn calibration target at the beginning and end of the session. The spectrum from each run was stored on the computer for later analysis.

From the first thin-film Mn calibration spectrum we observed the dominant Mn K_α peak at around channel 230 (~ 5.9 keV in Figure 7). In the final Mn calibration spectrum taken at the end of the

Figure 5. *XRF set up for one run of sample SI-1963b, Sand Island, Utah.*

Figure 6. *"Dancing Bear" panel near Moab, Utah.*

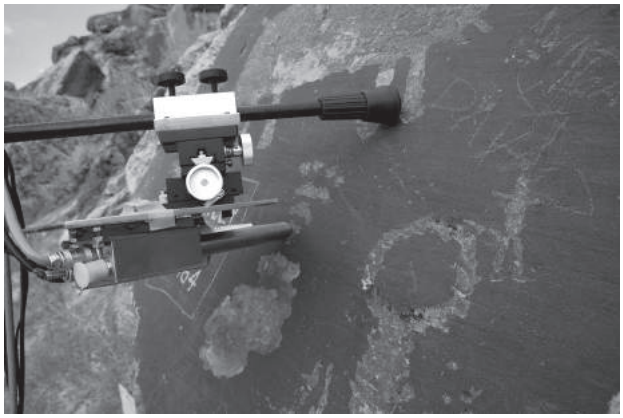

Figure 7. *Close up of XRF device taking data of the "Dancing Bear" panel near Moab, Utah.*

day, we noted that the Mn K-alpha peak dropped approximately 7 channels (0.18 keV) due to temperature-induced drift of the amplifier through the day. However, the gaussian widths were 7.0 channels for both spectra so the resolution of the instrument was not significantly affected by the temperature and a simple shift transformation will allow the spectra from the various runs to be accumulated.

Sample SI-1963c–d. The second set of glyphs we measured, identified here as SI-1963c-d, is shown in Figure 5 along with the XRF head positioned to measure the background patina adjacent to the "1". These samples consist of modern graffiti, SI-1963c (the "1" of the "1963" graffito) superimposed on a lizard petroglyph, SI-1963d, of perhaps a Pueblo I-II style (AD 750–1150).

We took three 900-second measurements along the ~1cm width of the "1" in the "1963" graffito, and four additional 900-second measurements in the "1" approximately 1 cm below the previous. We took two 900-second measurements in the tail region of the lizard petroglyph immediately above the "1." In addition we took three 900-second measurements of the background patina to the left and right of the lizard's tail as well as three 300-second measurements of the thin-film Mn slide. The spectrum from each run was stored in separate files on the computer for later analysis.

The "Dancing Bear" Panel. The "Dancing Bear" petroglyph panel, Figure 6, is located on BLM land north of Moab, Utah. This panel consists of modern graffiti immediately adjacent to petroglyphs of various styles. We took measurements of the "Harley Nelson\1964" graffito, and the adjacent "bear paw" and "lobe head" petroglyphs immediately to the right as seen in Figure 6 as well as another "lobe head" petroglyph located behind the main panel. We received permission to conduct the experiments from Leigh Grench of the BLM Field Office, Moab, Utah. Figure 7 shows a close up of the XRF device taking measurements of the bear paw petroglyph.

Sample DB-1964a ("Harley Nelson 1964" graffito). The first glyph measured, identified here as DB-1964a, shown in Figure 6, consists of a modern graffito ("Harley Nelson\1964") adjacent to several petroglyphs. We set up our apparatus following the procedure described in the previous section. We set the Mini-X to 15 kV and 100 μA. The higher current allowed faster data collection while still keeping the dead time below 4 percent. We took one 600-second measurement of each letter/number in the "Harley Nelson\1964" graffito using the XY-translation stage to position the x-ray beam accurately. We also took a 200-second measurement of the thin-film Mn calibration target at the end of the session as well as a 300-second measurement of the background patina near the "1." The spectrum from each run was stored on the computer for later analysis.

Sample DB-1964b ("bear paw" glyph). The next glyph measured, identified here as DB-1964b, was the (possibly) Ute-style bear paw located immediately to the right of the "Harley Nelson" graffito as shown in Figures 6 and 7. The Mini-X settings were the same as for sample DB-1964a. We took one 600-second measurement of the lower pad of the bear paw and stored the spectrum for later analysis.

Sample DB-1964c ("lobe head #1" glyph). The next glyph measured, identified here as DB-1964c, was the (possibly) archaic lobe-head figure located immediately to the right of the "bear paw" glyph as shown in Figures 6 and 7. The Mini-X settings were the same as for sample DB-1964a. We took one 600-second measurements of the foot region using the XY-translation stage to position the x-ray beam accurately. The spectrum from each run was stored on the computer for later analysis.

Sample DB-1964d ("lobe head #2", referred to as "solar deity" in the talk). The next glyph measured, identified here as DB-1964d, was the (possibly) archaic lobe-head figure located on a rock behind the main panel. The Mini-X settings were the same as for sample DB-1964a. We took one 600-second measurement in the region of the right arm as well as a 600-second measurement of the background patina immediately below the right arm of the petroglyph. The spectrum from each run was stored on the computer for later analysis.

DATA ANALYSIS

All data analysis was performed in *Mathematica* (Wolfram 1999). We wrote a subroutine to import the "SPE" formatted files stored by the Maestreo data acquisition software and used Mathematica's internal "FindFit" function to determine the fit parameters. The errors quoted are statistical only and were determined by a χ^2 analysis at the 90 percent confidence level.

Mn Calibration

In order to convert XRF data into absolute Mn surface densities, we used a thin-film Mn standard target created by Dr. Joseph Beach who deposited on a glass slide 158 nm as determined from profilometer and independent commercial XRF measurements. Figure 8 shows one XRF spectrum for this target with the x-ray source set at 15 kV and 60 μA.

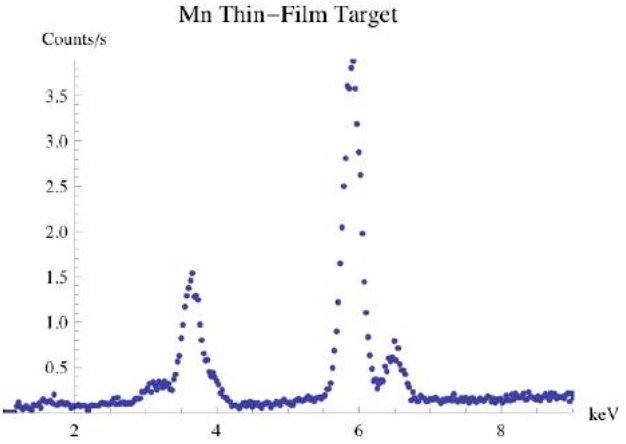

Figure 8. *XRF spectrum of the thin-film Mn calibration target.*

To determine the calibration constant needed to convert count rate into Mn surface density, we perform a linear background subtraction using the background spectrum to the immediate left and right of the Mn peaks. We adjust the background fit channels to give a minimum slope and intercept. Following background subtraction, we fit the residual spectrum in the Mn $K_{\alpha/\beta}$ peak region to the sum of two gaussians. We then use the K_α peak area to compute a calibration constant that can be used to convert Mn K_α count rate for any sample measurement to an absolute Mn surface density. The mass attenuation factor for 6 keV x-rays is 74.2 cm^2 /g (Tertian and Claisse 1982), giving an attenuation length in Mn of approximately 18 μm which is much greater than the film thickness. Therefore, the Mn peak area will be directly proportional to the thickness. Specifically, the surface density of Mn in a sample experiment giving a peak count rate of R_σ is given by: $\sigma = t_0 \rho_0 R_\sigma/R_0$, where t_0= 158 nm = 15.8 x 10^{-6} cm, μ_0 = 7.47 x 10^6 ρg/cm^3, where R_0 is the Mn K_α peak count rate for the thin-film calibration standard and R_σ is the Mn K_α peak count rate for the sample. With the units and values used here, σ will be in μg/cm^2.

Lytle et al. (2009) have measured Mn levels in petroglyphs and have calibrated Mn levels to dates using independent cosmogenic and geological data. Since the published Lytle, et al. calibration curve is not given in absolute manganese densities and is dependent on the experimental details of their equipment and protocols, we cannot use it directly for our measurements. In order to provide a basis for comparison, we provided Dr. Lytle with the same 158 nm Mn thin-film calibration slide used above. For this sample he measured a Mn peak area that would be equivalent to an age of 15,400 years based on his calibration curve. From this information we determine the slope of the Lytle, et al., calibration line to be 130.5 years/ (μg-Mn/cm^2) (Farrell Lytle, personal communication 2009).

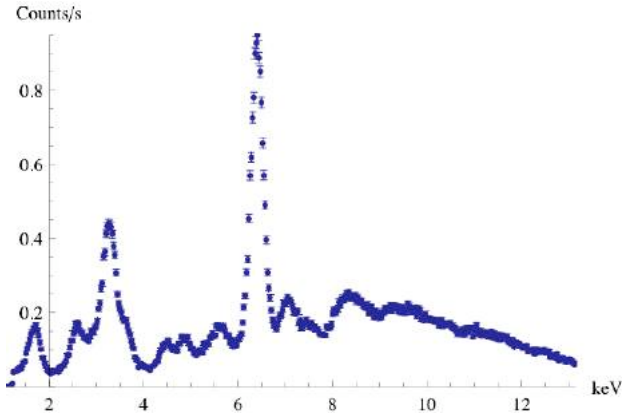

Figure 9. *XRF spectrum of Sand Island base rock. The base rock at the "Dancing Bear" site produced a similar spectrum.*

Base Rock Data

Sand Island Base Rock. The next step in the data analysis is to measure the Mn level in the base rock underlying the desert varnish. While at the Sand Island site, we collected a small (marble-sized) piece of base rock that had spalled from the rock face in the vicinity of the petroglyphs. After returning from the field, we trimmed the sample to ensure no influence of surface contaminants and performed long count-time XRF measurements of the sample.

Figure 9 shows one of our XRF spectra of the Sand Island base rock. We believe the peak at approximately 5.6 keV is due to Samarium which is in the same group of the periodic table as iron. The Sm L_α (L_β) peaks, at 5.64 keV (6.21 keV), are close enough to the Mn peaks to give a false positive Mn result if not accounted for; therefore we fit both the Mn and Sm peaks simultaneously in our analyses. From this analysis of the base rock spectrum described below, we determined that the manganese level in the base rock was consistent with zero, that is, below our detectable limits. On the other hand, as we see from Figure 9, we found a clear Sm peak with a peak height of about 0.04 counts/s with background subtraction (~0.16 counts/s with background).

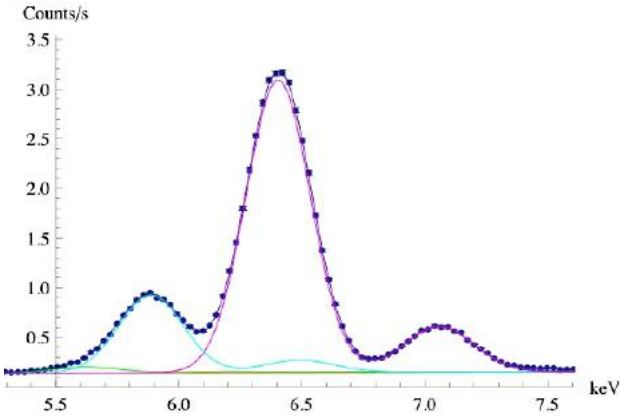

Figure 10. *XRF spectrum of the big-horn sheep petroglyph for sample SI-1963a-b. The above-background contributions for Sm, Mn and Fe are given by green, cyan, and red lines, respectively. The blue line is the sum.*

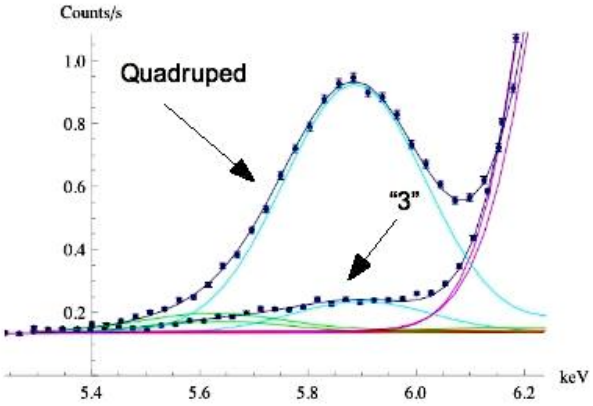

Figure 11. *Close-up of the XRF spectra in the Mn energy region for both the "3" graffito and the quadruped in samples SI-1963a-b. The above-background contributions for Sm, Mn and Fe are given by green, cyan, and red lines, respectively. The blue line is the sum.*

"Dancing Bear" Site Base Rock. In a similar fashion to the procedure followed at Sand Island, while at the "Dancing Bear" site, we collected a small (marble-sized) piece of base rock that had spalled from the rock and made a long measurement in the lab. The XRF spectra of the "Dancing Bear" site base rock was essentially identical to that of Sand Island (Figure 9) including a Samarium peak at about 5.6 keV. Therefore, again we fit both the Mn and Sm peaks simultaneously in our analyses. However, unlike the Sand Island base rock, we found a small residual Mn level of approximately 0.33 +/- 0.13 μg-Mn/cm^2 , close to our detectable limit. In the results presented below, this value is subtracted from the petroglyph/graffiti values to determine the Mn level in the desert varnish alone.

Fitting Procedure

Figure 10 shows an example XRF spectrum in the Mn/Fe energy region for sample SI-1963b ("Big-horn sheep" petroglyph) just above the "3" of the "1963" graffito taken at the Sand Island, Utah, the "3" graffito, sample SI-1963a ("1963"), and the quadruped petroglyph, sample SI-1963-b (see Figure 4). Also shown are our fits to the spectrum broken down by contributions from the various elements analyzed, Sm, Mn, and Fe.

The analysis procedure consists of five steps:

1. Since all spectra taken include dominant Fe peaks, we use these to calibrate the energy. Focusing on the Fe $K_{\alpha,\beta}$ region, we perform a linear background subtraction and then fit the Fe K_α and K_β peaks only using a sum of gaussians. From these fits we calibrate the energy as a function of channel, compute the widths, and the ratio of K_β to K_α.
2. Focusing on the Mn and Sm energy region, after background subtraction, we fit this region to a sum of gaussians with the centroids, widths, and β-to-α peak height ratios determined by the Fe fitting procedure described in step 1. This leaves only the Mn/Sm K_α peak heights to be determined by the data.
3. Since the Mn K_β peak lies under the Fe K_α peak, if the Mn K_α peak height is greater than about 10 percent of the Fe K_α peak, we re-fit the Fe peaks after subtracting the Mn K_β contribution. We find a single iteration is sufficient to produce a stable set of fit parameters.
4. From the Mn K_α peak height and width, using the Mn calibration constant, we determine the Mn

Table 1. *Manganese surface densities and estimated age for Sand Island samples.*

Sample	Mn (μg/cm^2) "Age" (yBP)(Lytle)	χ^2/df		"Age" (yBP) (linear model)
SI-1963a ("3" graffito)	3.17 +/- 0.23	1.4		414
SI-1963b (Big-horn sheep glyph)	25.27 +/- 0.43	1.1	367 +/- 33 (9.1%)	3297
SI-1963c ("1" graffito)	3.05 +/- 0.49	1.3		398
SI-1963d (Lizard glyph)	25.52 +/- 0.87	1.5	385 +/- 75 (19.6%)	3534

Table 2. *Manganese surface densities and estimated age for the "Dancing Bear" site samples.*

Sample	Mn (μg/cm^2) "Age" (yBP)(Lytle)	χ^2/df		"Age" (yBP) (linear model)
DB-1964a "Harley Nelson1964"	2.49 +/- 0.59	1.4		
DB-1964a background patina	52.73 +/- 1.33	2.0		
DB-1964b "Bear paw"	33.23 +/- 0.65	1.4	607 +/- 156	4340
DB-1963c "Lobe head #1"	51.02 +/- 1.6	1.5	931 +/- 251	6660
DB-1964d "Lobe head #2"	51.93 +/- 1.1	1.5	948 +/- 245	6750
DB-1964d background patina	86.57 +/- 1.2	1.6		

surface density as described in the Mn calibration subsection above..

5. For each set of fit parameters we calculated a χ^2 per degree of freedom and by varying the fit parameters around the best fit values determined errors at the 90 percent confidence level (statistical only).

RESULTS

Sand Island samples SI-1963a-b

We carried out the fitting procedure described in Section VI.C. for the measurements of samples SI-1963a-b. In addition, for each case a separate thin-film Mn calibration spectrum was taken to provide the calibration factor needed to convert these count rates to absolute Mn surface density as described in Section VI.A. The results of our analyses for samples SI-1963a-b are given in Table 1.

As seen in Figures 10 and 11, the quality of the fits is excellent with a χ^2 per degree of freedom ranging from 1.–1.5. The errors quoted represent a 90 percent confidence level for the value of the measurement reported. It was initially puzzling that the background patina adjacent to samples SI-1963a-d actually had less Mn (24.2 mg/cm^2) than in the petroglyphs. The puzzle was resolved when a close examination of the background revealed that it had been subjected to high-point abrasion which removed significant amounts of desert varnish resulting in the lower Mn levels.

Dancing Bear Panel samples DB-1964a-d

We carried out the fitting procedure described in Section VI.C. for the measurements of samples DB-1964a-d. In addition, for each case a separate thin-film Mn calibration spectrum was taken to provide the calibration factor needed to convert these count rates to absolute Mn surface density as described in Section VI.A. The results of our analyses for samples DB-1964a-d are given in Table 2 along with estimated ages based on a linear extrapolation from the graffiti compared with the dates using the Lytle et al. calibration.

The background patina on the main panel in the region in the vicinity of the graffiti (sample DB-1964a) had significantly less Mn than that adjacent to sample DB-1964d ("Lobe head #2") behind the main panel. On close examination there appeared to be some abrasion of the back-

ground in the vicinity of the graffiti which could have reduced the Mn level there, but further study is needed.

SUMMARY AND CONCLUSIONS

We have constructed a portable XRF device for field deployment that enables one to count for long periods of time with the goal of detecting low levels of manganese in petroglyphs and graffiti. We used this device to measure Mn levels in petroglyphs and graffiti at Sand Island outside of Bluff, Utah, and at the "Dancing Bear" panel north of Moab, Utah. For the first time, we have measured Mn surface densities in graffiti representing the earliest stages of repatination.

To convert the measured manganese levels to an age requires a model of how the manganese accumulates as a function of time. The simplest model is to take a linear accumulation rate as assumed by Lytle et al. For the Sand Island samples, SI-1963a-d, we determined that about 3.1 $\mu g/cm^2$ of Mn has accumulated in the "1963" graffito since its creation giving a Mn accumulation rate of 0.076 $\mu g/cm^2$ per year or, equivalently stated, it takes 14.8 years to accumulate one $\mu g/cm^2$ of Mn. For the "Dancing Bear" site samples, DB-1964a-d, we determined that about 2.5 $\mu g/cm^2$ of Mn has accumulated in the "1964" graffito since its creation giving a Mn accumulation rate of 0.056 mg/cm^2 per year (18 years to accumulate one $\mu g/cm^2$ of Mn). Both of these Mn accumulation rates are significantly greater than those reported by Lytle et al. who find a Mn accumulation rate of only 0.0077 $\mu g/cm^2$ per year (or, 130 years to accumulate one $\mu g/cm^2$ of Mn). Resolving the discrepancy with the Lytle et al. calibration will require cross calibrating the same sources.

Based on the Mn measurement in the petroglyphs at each site, *assuming* a linear model for Mn accumulation, we calculate an age of 367 +/- 33 (9.1%) years for the lizard petroglyph, sample SI-1963d, shown in Figure 5. However, if this is indeed a Pueblo I or II style petroglyph based on its subject and style, we would expect an age of around 900 to 1300 years, (Cole 2009). Likewise, we find an age of 385 +/- 75 (19.6%) years for sample SI-1963b, the big-horn sheep petroglyph shown in Figure 4. If we believe this petroglyph to be Archaic based on its subject and style, we would expect a much older age, perhaps as old as 3000–4000 years, (Cole 2009), and closer to the Lytle et al. values.

Similarly, for the "Dancing Bear" site, based on the linear accumulation model, sample DB-1964b, the age of the "bear paw" petroglyph is found to be approximately 607 +/- 156 years B.P. Similarly, the age of sample DB-1964-c, "lobe head#1" petroglyph is found to be 931 +/- 251 years B.P. The age of sample DB-1964d, the "lobe head#2" petroglyph (behind the main panel) is found to be 948 +/- 245 years B.P. With the significant discrepancy between the calculated dates based on Mn levels and that based on style, we suspect that the linear accumulation model, at least for the time spans covered in this study, may be too simplistic. It is encouraging that the two "lobe head" figures are measured to have approximately the same Mn levels although in different locations and orientations. The Mn accumulation history is apparently similar for both rock faces even though the background patina provided different Mn levels probably due to abrasion of the patina on the front panel.

We further note that the Mn levels for the two Sand Island graffiti are nearly the same to within experimental error even though they are on different regions of the rock which showed some variation in patination. This may not be surprising; however we also note that the two petroglyphs, supposedly of different ages based on the styles, also have approximately the same level of Mn. This observation suggests that perhaps there may be a rate-limiting factor in desert varnish accumulation providing further suggestion that the Mn accumulation may not be linear. It is hoped that this work will stimulate further investigation

Table 3. *Simulated time-lapse sequence for the "Dancing Bear" site near Moab, Utah, illustrating the potential for relative dating using XRF.*

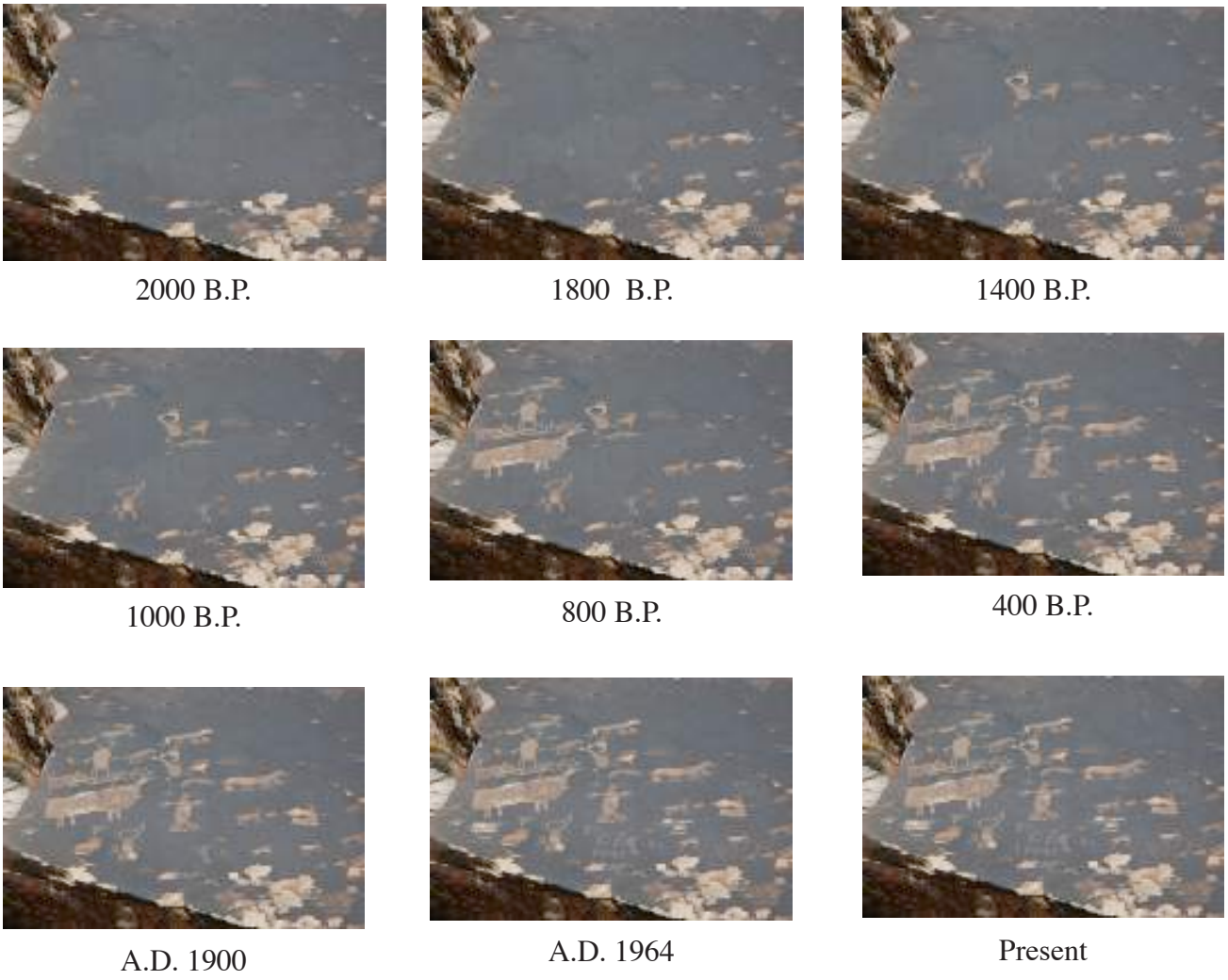

leading to a more sophisticated mathematical model for Mn accumulation rates. To constrain a nonlinear Mn accumulation model, it will be necessary to obtain more than one independently dated glyph. This will be the challenging subject of future work.

Finally, while absolute date calibration continues to present a challenge, the possibility of using Mn measurements to determine relative ages may still prove useful. By measuring the Mn level in each petroglyph of a site of multiple settlements over time, it may be possible to estimate the relative ages of the petroglyphs allowing one to create a time-lapse movie of the petroglyph site. Table 3 displays a *simulation* of a time-lapse of the "Dancing Bear" panel based upon hypothetical Mn levels.

Acknowledgements. We thank Winston Hurst for inviting us to conduct the study of petroglyphs in the Bluff, Utah, area, providing archaeological oversight of the project, showing us several candidate sites, and for partial support through the Comb Ridge Heritage Initiative Project, University of Colorado under contract to the BLM (Catherine M. Cameron, Principal Investigator). We thank Laura Kochanski of the Monticello BLM Field Office and Leigh Grench of the Moab BLM Field Office for permission to perform the

experiments, Joseph Beach for creating our Mn calibration target, Farrel Lytle for independent measurements of the Mn thin-film target, F. Edward Cecil for collaborations and assistance in the work at Sand Island, and Lynda McNeil for assisting with logistics and providing valuable background on the rock art of the region.

REFERENCES CITED

Beck, W. D., D. J. Donahue, A. J. T. Jull, G. Burr, W. S. Broecker, G. Bonani, I. Hajdas, and E. Malotki
1998 Ambiguities in Direct Dating of Rock Surfaces Using Radiocarbon Measurements. *Science* 280:2132–2139.

Cole, Sally J.
2009 *Legacy on Stone,* Johnson Books, Boulder, Colorado.

Dorn, Ronald I.
1989 Cation-Ratio Dating of Rock Varnish: A Geographical Perspective. *Progress in Physical Geography* 13:559–596.
1994 Dating Petroglyphs with a Three-Tier Rock Varnish Approach. In *New Light on Old Art: Recent Advances in Hunter-Gatherer Rock Art Research*, edited by David S. Whitley and Lawrence L. Loendorf, pp. 13–36. Monograph No. 36, Institute of Archaeology, University of California, Los Angeles.
1998a Age Determination of the Coso Rock Art. In *Coso Rock Art: A New Perspectiv*e, edited by Elva Younkin, pp. 67–96. Maturango Press. Ridgecrest, California.

Dorn, Ronald I. (continued)
1998b Response to Beck et al. *Science* 280:2132–2139.
2007 Rock Varnish, Chapter 8 in *Geochemical Sediments and Landscapes*, edited by David J. Nash and Sue J. McLaren. Blackwell, London.

Dorn, Ronald I., and T. M. Oberlander
1981 Microbial Origin of Desert Varnish. *Science* 213:1245–1247.

Francis, Julie E., and Lawrence L. Loendorf
2002 *Ancient Visions: Petroglyphs and Pictographs of the Wind River and Bighorn Country, Wyoming and Montana*, University of Utah Press. Salt Lake City, Utah.

Lytle, Farrell, Manetta Lytle, Alexander Rogers, Alan Garfinkel, Caroline Maddock, William Wight, and Clint Cole
2008 An Experimental Technique for Measuring Age of Petroglyph Production: Results on Coso Petroglyphs. Paper presented at the 31st Great Basin Anthropological Conference, Portland, Oregon.

Tertian, R., and Claisse, F.
1982 *Principles of Quantitative X-ray Fluorescence Analysis,* Heyden and Son, Ltd., London.

Wolfram, Stephen
1999 The Mathematica Book, fourth edition, Cambridge University Press, Cambridge, UK. (http://www.wolfram.com/products/mathematica/index.html).